Available online at www.sciencedirect.com
ScienceDirect
Trans. Nonferrous Met. Soc. China 20(2010) s393−s396
Transactions of Nonferrous Metals Society of China
www.tnmsc.cn

Effect of cooling rates on as-cast microstructures of Mg-9Al-*x*Si (*x*=1, 3) alloys

LI Xin-lin(李新林)[1, 2], CHEN Yan-bin(陈彦宾)[1], WANG Xiang(王 香)[2], MA Guo-rui(马国睿)[2]

1. College of Materials Science and Engineering, Harbin Institute of Technology, Harbin 150001, China;
2. Centre for Biomedical Materials and Engineering, College of Materials Science and Chemical Engineering, Harbin Engineering University, Harbin 150001, China

Received 23 September 2009; accepted 30 January 2010

Abstract: The effects of cooling rates corresponding to different diameters of the steel mould and laser surface melting (LSM) on the as-cast microstructures of Mg-9Al-*x*Si (*x*=1, 3) (mass fraction, %) alloys were investigated by XRD and OM. The results show that obvious refinement of the alloy microstructure is obtained with increasing cooling rate by conventional ingot metallurgy. However, no evident modified morphologies of both dendritic primary Mg_2Si and Chinese script eutectic Mg_2Si in the Mg-Al-Si alloy occurs. Surprisingly, the morphologies of Mg_2Si phases within the laser-melted Mg-Al-Si alloy transform drastically from both coarse Chinese script shape for the eutectic Mg_2Si and dendrite for the primary Mg_2Si to fine spherical particles with an average size of about 3 μm due to the rapid cooling of the melted layer, and the Mg_2Si particulates distribute more uniformly in the *α*-Mg matrix.
Key words: Mg-Al-Si alloys; Mg_2Si; modification; cooling rates; microstructure

1 Introduction

Mg-Al based alloys such as AZ91 are the most widely used magnesium alloys for structural applications, for their excellent castability and good strength. However, Mg-Al based alloys have poor creep resistance due to the thermal instability of $Mg_{17}Al_{12}$ phases[1−2]. The most common way of improving the high-temperature properties of magnesium is to induce formation of thermally stable precipitates or dispersoids as barriers to pin dislocation movement, e.g. cross slip or dislocation climb[3]. Si is an effective alloying element for such purpose since the addition of Si to Mg alloys combines with Mg to form the intermetallic compound Mg_2Si which exhibits high melting temperature, low density, high hardness and low thermal expansion coefficient[4]. Thus, Mg-Al-Si based alloys have high potential as heat resistant light metals due to the excellent combination of various properties, which mainly depends on the morphology and size of Mg_2Si. However, the Mg-Al-Si based alloy showed very low ductility and strength due to the formation of the coarse dendrite-shape primary Mg_2Si in Mg-Si alloys with high Si content and the brittle Chinese script eutectic Mg_2Si in Mg-Si alloys with low Si content during slow cooling [5−6]. It is widely known that the refinement of microstructure is mainly responsible for the improvement in the mechanical properties[7−8]. The scale of the microstructure is directly influenced by the cooling rate. Generally, rapid solidification, such as melt-spinning, spray atomization and rapid quenching [9−10], can greatly enhance the mechanical properties over conventional processing alloys of the same composition through the extension of solid solubility limits, the refinement of microstructure and the dispersion of second phase[11−12]. However, few investigations were carried out on the effect of the cooling rate on the microstructures of Mg-Al-Si alloys. The purpose of the present work is to study the as-cast microstructural evolution of the Mg-9Al-*x*Si (*x*=1, 3) alloys at different cooling rates.

2 Experimental

Mg-9Al-*x*Si (*x*=1, 3) (mass fraction, %)alloys were

Foundation item: Project(LRB05-311) supported by the Postdoctoral Foundation of Heilongjiang Province, China; Project(HEUFT05038) supported by the Basic Research Foundation of Harbin Engineering University, China; Project(2009AA03Z423) supported by the National High-Tech Research and Development Program of China
Corresponding author: LI Xin-lin; Tel.:+86-451-82518173; Fax:+86-451-82518644; E-mail: lixinlin@hrbeu.edu.cn

prepared. Commercially pure Mg, Al and Si were melted in a graphite crucible in an electric resistance furnace under the protection of a RJ-2 covering flux. The melt was stirred to assist the dissolution of the alloying elements, and then was poured into cylinder steel moulds with different diameters of 5, 10 and 25 mm after holding at 780 ˚C for about 50 min. Subsequently, Mg-9Al-*x*Si (x=1, 3) alloys with dimensions of d25 mm× 10 mm were surface remelted by laser. The laser was employed at a scanning speed of 1.4 mm/s processing a pulse width of 25 ms, repetition frequency of 55 Hz, and pulse energy of 7 J. Ar was provided as protective gas at a pressure of 0.3 MPa. The chemical compositions of the alloy were measured with an ARL 4460 Metals Analyzer, as shown in Table 1. Metallographic samples were prepared in accordance with standard procedures, and etched with 3% HNO_3 in alcohol. Microstructure and phase analyses were investigated by optical microscopy (OM) (Axiovert 200 MAT, Germany) and X-ray diffractometry (XRD) (X’Pert PRO, Holand), respectively.

Table 1 Chemical composition of Mg-9Al-*x*Si (x=1, 3) alloys used in this study (mass fraction, %)

Alloy	Al	Si	Zn	Cu
Mg-9Al-1Si	8.116 73	0.827 20	0.011 65	0.000 89
Mg-9Al-3Si	8.216 20	3.181 87	0.009 73	0.000 41

Alloy	Fe	Ni	Mg
Mg-9Al-1Si	0.004 56	0.001 19	Bal.
Mg-9Al-3Si	0.010 77	0.001 44	Bal.

3 Results and discussion

3.1 Phase constituents

Fig.1 shows the XRD patterns of Mg-9Al-*x*Si (x=1, 3) alloys. There are α-Mg, β-$Mg_{17}Al_{12}$ and Mg_2Si phases in both the Mg-9Al-1Si alloy and Mg-9Al-3Si alloy, which agrees with the Mg-Al-Si ternary phase diagram [12].

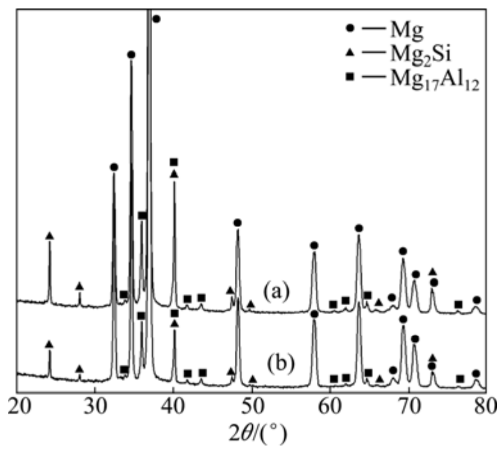

Fig.1 XRD patterns of Mg-9Al-Si alloys: (a) Mg-9Al-1Si; (b) Mg-9Al-3Si

3.2 Microstructure of Mg-Al-Si alloys

3.2.1 Effect of composition on microstructure

Figs.2(a) and (b) show the typical as-cast micro-structures of Mg-Al-Si alloys. It can be seen that the as-cast microstructures of the Mg-9Al-1Si alloys comprise α-Mg dendrites, (α-Mg+Mg_2Si) eutectic with Chinese script Mg_2Si embedded in the α-Mg matrix and β-$Mg_{17}Al_{12}$ precipitated discontinuously at grain boundaries; while that of the Mg-9Al-3Si alloys consist of not only the three phases mentioned above, but also Mg_2Si primary dendrites that are surrounded by α-Mg sub-primary particles[13].

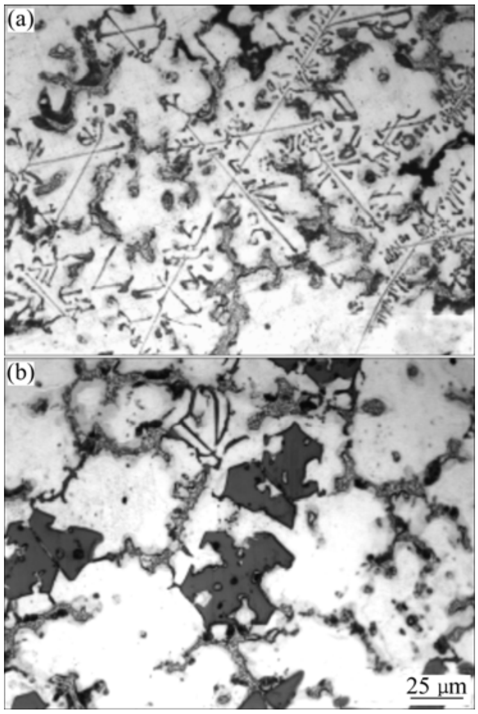

Fig.2 As-cast microstructures of Mg-Al-Si alloys: (a) Mg-9Al-1Si; (b) Mg-9Al-3Si

3.2.2 Effect of cooling rate on microstructure

Figs.3 and 4 show that microstructures of the Mg-9Al-*x*Si (x=1, 3) alloys at different cooling rates, different diameters of the steel mould and laser surface melting (LSM), respectively. From Figs.3(a)−(c) and Figs.4(a)−(c), there are obvious refinement of the alloy microstructure with increasing cooling rate by conventional ingot metallurgy. However, no evident modification of the morphologies of Chinese script eutectic Mg_2Si in the Mg-9Al-1Si alloy occurs, while the structure of primary Mg_2Si in the Mg-9Al-3Si alloy changes from equiaxial dendrites to a dendrite configuration. It should be mentioned that eutectic Mg_2Si phases partially precipitate in the interdendritic region of the primary α-Mg phases due to the interdendritic

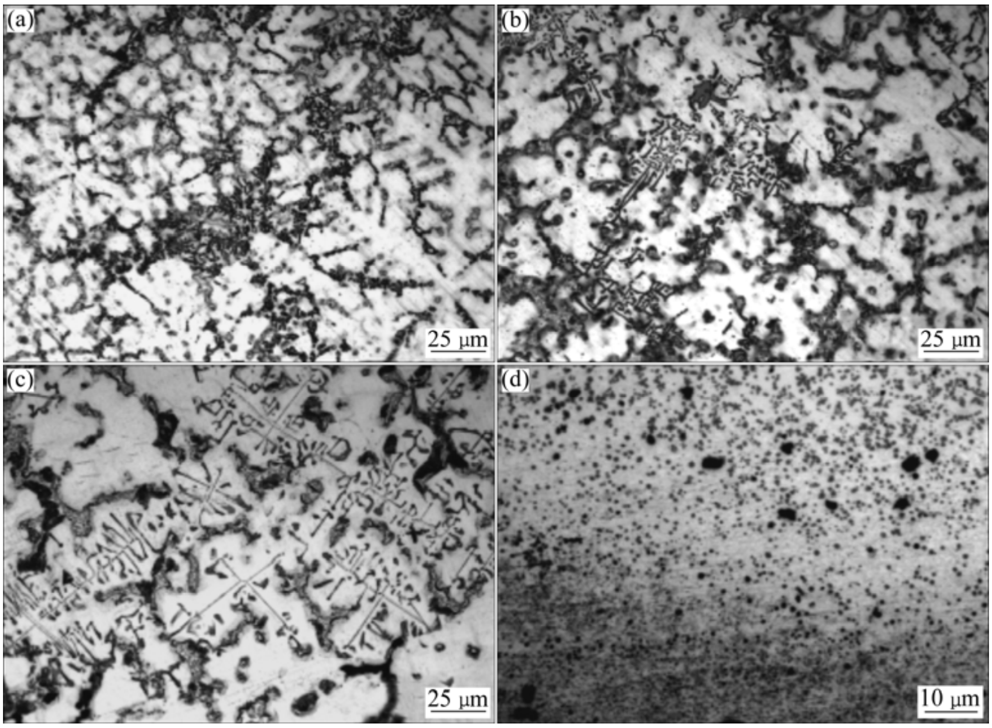

Fig.3 Optical microscopy microstructures of Mg-9Al-1Si alloys with different diameters of steel mould ((a) 5 mm; (b) 10 mm; (c) 25 mm) and LSM treatment (d)

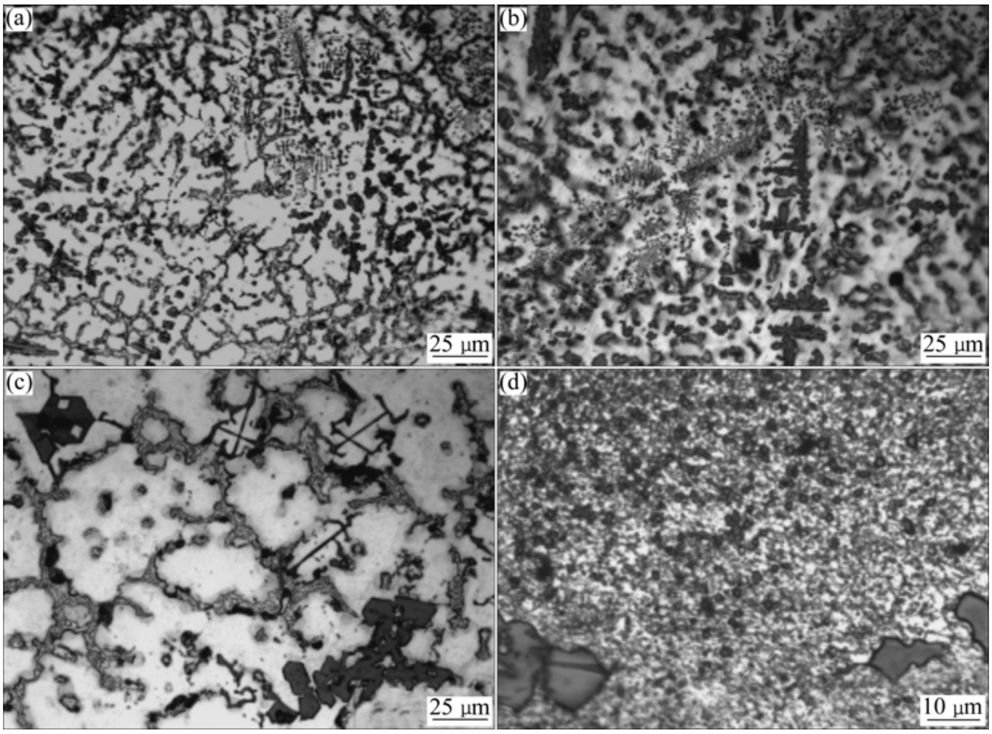

Fig.4 Optical microscopy microstructures of Mg-9Al-3Si alloys with different diameters of steel mould ((a) 5 mm; (b) 10 mm; (c) 25 mm) and LSM treatment (d)

segregation caused by relatively rapid cooling. Surprisingly, it can be seen from Figs.3(d) and (d) that the morphologies of Mg_2Si phases in the laser-melted Mg-Al-Si alloy transforms drastically from both coarse Chinese script eutectic Mg_2Si and dendritic or equiaxial primary Mg_2Si to fine spherical particles with an average size of about 3 μm due to a high degree of undercooling resulting from the rapid cooling of the laser-melted layer by LSM[14−15], which results in more uniform distribution of the Mg_2Si particulates in the α-Mg matrix.

4 Conclusions

1) Obvious refinement of the microstructures of the Mg-9Al-*x*Si (*x*=1, 3) alloys was obtained by increasing the cooling rate of conventional ingot metallurgy. However, there is no obvious modification of the morphologies of dendrite-shape primary Mg_2Si and Chinese script eutectic Mg_2Si in the Mg-Al-Si alloy.

2) The morphologies of Mg_2Si phases in the Mg-Al-Si alloy processed by LSM transforms drastically from both coarse Chinese script for the eutectic Mg_2Si and dendrites for the primary Mg_2Si to fine spherical particles with an average size of about 3 μm, and fine Mg_2Si particulates distribute more uniformly in the α-Mg matrix in the laser melted layers.

References

[1] BLUM W, ZHANG P, WATZINGER B, GROSSMANN B V, HALDENWANGER H G. Comparative study of creep of the die-cast Mg-alloys AZ91, AS21, AS41, AM60 and AE42 [J]. Materials Science and Engineering A, 2001, 319/321: 735−740.

[2] JUNG I H, KANG D H, PARK W J, KIM N J, AHN S H. Thermodynamic modeling of the Mg-Si-Sn system [J]. Computer Coupling of Phase Diagrams and Thermochemistry, 2007, 31: 192−200.

[3] KANG D H, PARK S S, KIM N J. Development of creep resistant die cast Mg-Sn-Al-Si alloy [J]. Materials Science and Engineering A, 2005, 413/414: 555−560.

[4] KIM J J, KIM D H, SHIN K S, KIM N J. Modification of Mg_2Si morphology in squeeze cast Mg-Al-Zn-Si alloys by Ca or P addition [J]. Scripta Materialia, 1999, 41(3): 333−340.

[5] ZHENG Na, WANG Hui-yuan, WANG Wei, GU Zhen-hua, LI Dong, JIANG Qi-chuan. Invalidation of KBF_4 modification on the primary Mg_2Si in Mg-Si alloys by Al addition [J]. Journal of Alloys and Compounds, 2008, 459(1/2): L8−L12.

[6] DU Jun, IWAI K, LI Wen-fang, PENG Ji-hua. Effects of alternating current imposition and alkaline earth elements on modification of primary Mg_2Si crystals in hypereutectic Mg-Si alloy [J]. Transactions of Nonferrous Metals Society of China, 2009, 19(5): 1051−1056.

[7] WANG Hui-yuan, WANG Wei, ZHA Min, ZHENG Na, GU Zhen-hua, LI Dong, JIANG Qi-chuan. Influence of the amount of KBF_4 on the morphology of Mg_2Si in Mg-5Si alloys [J]. Materials Chemistry and Physics, 2008, 108(2/3): 353−358.

[8] LU L, THONG K K, GUPTA M. Mg-based composite reinforced by Mg_2Si [J]. Composites Science and Technology, 2003, 63(5): 627−632.

[9] SAMANT A N, DU B S, PAITAL S R, KUMAR S, DAHOTRE N B. Pulsed laser surface treatment of magnesium alloy: Correlation between thermal model and experimental observations [J]. Journal of Materials Processing Technology, 2009, 209(11): 5060−5067.

[10] MAJUMDAR J D, GALUN R, MORDIKE B L, MANNA I. Effect of laser surface melting on corrosion and wear resistance of a commercial magnesium alloy [J]. Materials Science and Engineering A, 2003, 361(1/2): 119−129.

[11] XU Chang-lin, WANG Hui-yuan, QIU Feng, YANG Ya-feng, JIANG Qi-chuan. Cooling rate and microstructure of rapidly solidified Al-20wt. % Si alloy [J]. Materials Science and Engineering A, 2006, 417(1/2): 275−280.

[12] LIU Chu-ming, ZHU Xiu-rong, ZHOU Hai-tao. Phase diagram collection of magnesium alloys [M]. Changsha: Central South University Press, 2006: 139−140. (in Chinese)

[13] PAN Yi-chuan, LIU Xiang-fa, YANG Hua. Microstructural formation in a hypereutectic Mg-Si alloy [J]. Materials Characterization, 2005, 55(13): 241−247.

[14] ABBAS G, LIU Z, SKELDON P. Corrosion behaviour of laser-melted magnesium alloys [J]. Applied Surface Science, 2005, 247: 347−353.

[15] DUBÉ D, FISET M, COUTURE A, NAKATSUGAWA I. Characterization and performance of laser melted AZ91D and AM60B [J]. Materials Science and Engineering A, 2001, 299(1/2): 38−45.

(Edited by FANG Jing-hua)